

Toward A Non-Prestressed Precast Long-Span Bridge Girder Using UHP-FRC

Shih-Ho Chao^(a), Venkatesh Kaka^(b), and Missagh Shamshiri^(c)

(a) Professor of Civil Engineering, the University of Texas at Arlington, Arlington, Texas

(b) Project Engineer, Armstrong-Douglass Structural Engineers, Dallas, Texas

(c) Graduate student, the University of Texas at Arlington, Arlington, Texas

Abstract: The exceptional compression strength and ductility of ultra-high-performance fiber-reinforced concrete (UHP-FRC) can revolutionize the design of reinforced concrete structural members. While the maximum useable compressive strain, ϵ_{cu} , for conventional plain concrete is assumed to be 0.003 in current design codes (ACI 318 Building Code and AASHTO LRFD Bridge Design Specifications), UHP-FRC's ϵ_{cu} is 5 to 10 times higher. Underestimating the compressive ductility of UHP-FRC limits the allowable maximum amount of longitudinal reinforcement, which in turn leads to limited flexural capacity of the members. Conventional reinforced concrete members are designed with a smaller amount of reinforcement to meet tension-controlled behavior. This design approach in turn leads to 1) a small ultimate flexural capacity, 2) a large amount of cracking and wider crack widths under service loads, which lead to a reduced member stiffness, 3) cracks that are less likely to close after overloading, 4) a small compression zone depth that allows cracks to propagate deeply, which further reduces the stiffness, 5) large strains in rebars, which reduce aggregate interlock and shear strength, and 6) considerable yielding of rebars, which causes bond deterioration. Contrary to the conventional design concept, a new ductile-concrete strong-reinforcement (DCSR) design concept is investigated in this study. A maximum useable compressive strain of 0.015 is considered for UHP-FRC, which allows a concrete member to maintain tension-controlled behavior while using a high amount of steel rebars. Accordingly, the flexural capacity of the section increases. This approach allows the UHP-FRC's high compressive strength to be effectively utilized in the compression zone. The synergistic interaction of strong steel and tensile strength of UHP-FRC considerably increases the cracking resistance of the member. In addition, the number and size of initial microcracks are limited due to the strong bridging effect of a high amount of steel. Therefore, the member maintains its stiffness and small deflection under service loads. This feature permits eliminating prestressing in bridge girders, where an uncracked section is desired under service loads. Besides experimental evidence, a prototype single-span 250-ft long non-prestressed UHP-FRC decked bulb-tee (DBT) girder was designed using the DCSR concept. Finite element analysis with AASHTO loading confirms that the new UHP-FRC girder satisfies code requirements. The experimental and analytical results show that conventional precast prestressed concrete girders can be replaced by the new non-prestressed decked UHP-FRC girders.

Keywords: UHP-FRC, long-span, high-strength steel, bridge, DBT, prestressed concrete

1. Introduction

1.1 Prestressed Concrete

Freyssinet (1936) summarized the advantages of using prestressed concrete as compared to conventional reinforced concrete as: 1) a considerable reduction of deformation (deflection), 2) complete suppression of cracks, 3) a decrease of the maximum compression stress in bending, 4) a decrease of tension produced in the concrete by the shear stresses, and 5) considerable resistance against repeated stressing. Since prestressed concrete does not crack under service loads, the entire section is generally active in resisting the load and provides effective deflection control, while in reinforced concrete only the uncracked part of the section is active (Naaman 2012). Together with the use of high-strength prestressing steel and concrete, prestressed concrete members are generally lighter. Also, it is often claimed that prestressed concrete has high resilience because the considerable elastic restoring force from the reinforcement can close the cracks temporarily developed due to overloading (Leonhardt 1964; Lin and Burns 1981).

On the other hand, prestressed concrete also has its disadvantages. The consequences of corrosion in prestressing steel are more severe than in mild steel reinforcement because of the presence of high-stress in the steel and the diameter of prestressing steel is relatively small (Naaman 2012). The production of precast, prestressed concrete members involves the use of special prestressing equipment, requiring a prestressing bed and skilled labor. Additionally, the prediction of long-term prestress losses is usually cumbersome and by no means accurate. The initial high stress in concrete can also require additional longitudinal mild steel reinforcement and debonding of strands at the ends of girders to control the cracking. Delivery of large prestressed structures and the cost of transportation usually eliminates the possibilities of a very long span and/or curved profile to be precast. Camber-related issues often pose challenges to designers, fabricators and contractors. One example is the prefabricated deck bulb tee (DBT) girders. Many state DOTs and the Federal Highway Administration (FHWA) are promoting accelerated bridge construction (ABC). Using a prefabricated DBT eliminates the need for constructing cast-in-place decks and, hence, provides the benefits of rapid construction, improved safety for construction personnel and the public, and improved structural performance and durability (NCHRP 2009); however, the use of DBT girders has been limited to relatively short-span and low-traffic bridges. One of the reasons is the large prestress-induced cambers, which require considerable on-site effort to line up skewed DBT girders to eliminate the deck profile problems.

2. Ultra-High-Performance Fiber-Reinforced Concrete (UHP-FRC) Material Properties

UHP-FRC was developed by changing the porous nature of conventional concrete through reducing dimensions of microcracking (or defects) in the concrete. The consequences of a very dense microstructure and low-water ratio results in enhanced compressive strength (Horii and Nemat-Nasser, 1985) and delayed liquid ingress (FHWA 2011). Furthermore, the addition of steel or synthetic fibers also improves the brittle nature of concrete by increasing the tensile cracking resistance, post-cracking strength, ductility, and energy absorption capacity. In terms of corrosion resistance, research has indicated that UHP-FRC has a much greater durability than conventional concrete due to its very dense microstructure (Ahlborn et al 2011). In addition, research carried out by Grubb et al (2007) indicates that steel reinforcing bars embedded in steel fiber-reinforced concrete are more resistant to corrosion than the reinforcing bars in conventional plain concrete. Further, corrosion concerns can be further reduced if the ASTM A1035 high-strength, corrosion-resistant, low-carbon chromium reinforcing bars are used along with UHP-FRC.

3. Structural Application by Utilizing UHP-FRC's Unique Properties

UHP-FRC offers a new way to design reinforced concrete flexural members due to its superior mechanical properties as compared to conventional concrete. Figure 1 shows measured strains of one UHP-FRC beam by a digit image correlation (DIC) system compared to that of a reinforced concrete (RC) beam. These strains represent an average of all strains within a 10-in. (254 mm) gauge length within the constant moment region. The UHP-FRC (3% steel fiber by volume) used in this study was developed at UT Arlington (Aghdasi et al 2016). As can be observed, the maximum usable compressive strains, ϵ_{cu} , of UHP-FRC and plain concrete is approximately 0.015 and 0.003, respectively. Notably, ACI 318 (ACI 2014) and AASHTO LRFD (AASHTO 2017) use 0.003 as the design maximum strain at the crushing of concrete. Due to this small strain capacity of plain concrete, only a small amount of longitudinal reinforcement can be used in order to ensure that the flexural member is tension-controlled. For a tension-controlled beam section, the tensile strain in the extreme tension reinforcement (closest to the tension face) must be sufficiently large (≥ 0.005); therefore, the beam shows a large deflection as a warning before failure occurs. If the concrete compressive strain can be 5 to 10 times greater, the beam could be more efficiently utilized by placing a considerably higher amount of longitudinal reinforcement while still maintaining tension-controlled behavior.

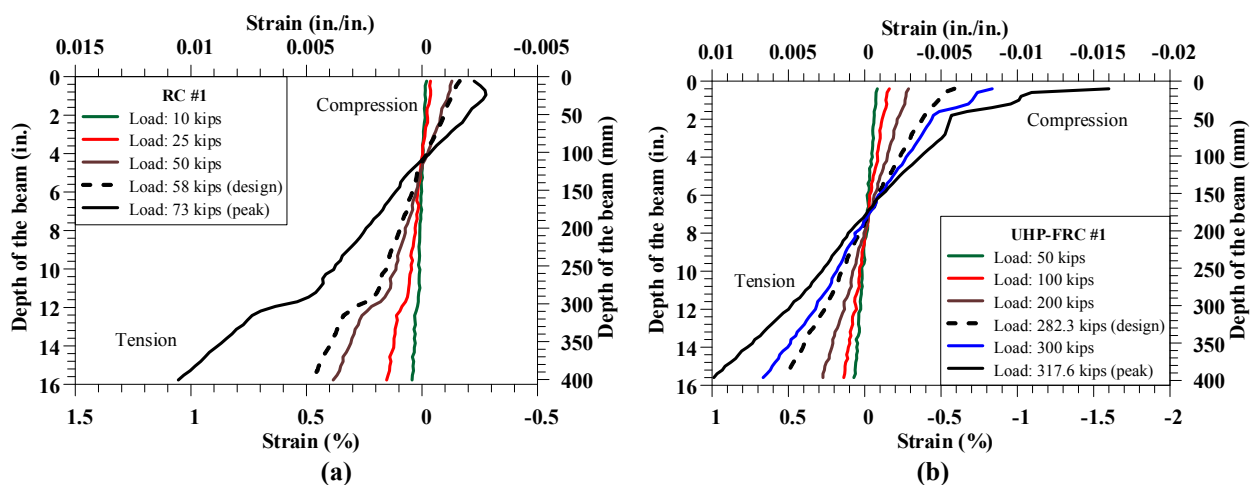
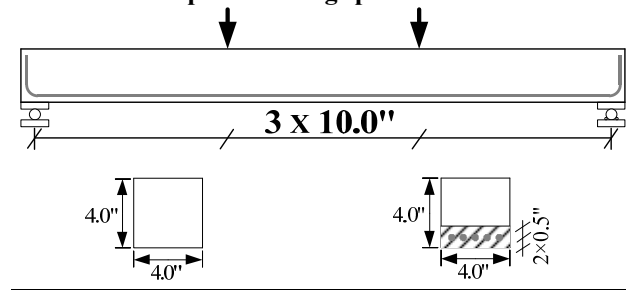


Figure 1. Average measured strains at various loads for the test beams by digit image correlation (DIC) measurement: (a) RC and (b) UHP-FRC #1

Prior research has shown that the presence of reinforcing bars in structural members enhances the cracking distribution and tensile ductility of steel fiber-reinforced concrete (SFRC) due to the tension-stiffening effect (Chao et al 2007; Aghdasi et al 2016). Therefore, adding a large amount of longitudinal reinforcement not only increases the flexural strength of UHP-FRC beams, but also enhances the mechanical behavior of UHP-FRC on the tensile side of the beam. Figure 2 shows a four-point loading testing of two small UHP-FRC beams for investigating the effect of the amount of reinforcement on the flexural cracking strength, f_r . The constant bending moment region between the two loading points is 10 in. (25.4 cm). The first specimen, R0, has no reinforcement and the second specimen R5 is reinforced with five #3 rebars (Table 1). A cracking-control longitudinal reinforcement ratio, ρ_{TA} , was calculated as the area of the reinforcement divided by a tributary area which is the product of the width of the beam by twice the cover (bottom concrete fiber to the center of the reinforcement). In both specimens, the flexural cracking occurred

prior to shear cracks. The first cracking load for each specimen is listed in Table 1 and highlighted in Figure 2. Test results show that increasing ρ_{TA} to 14% increased the first flexural cracking strength by 220%, from 1.5 ksi (10.3 MPa) to 3.3 ksi (22.8 MPa). This high cracking strength provides an effect similar to prestressing, which increases the first cracking strength of plain concrete (approximately 0.5 ksi to 0.75 ksi [3.4 MPa to 5.2 MPa]). While concrete's cracking strength can hardly be considerably increased in a typical RC member because the longitudinal reinforcement ratio is kept low to maintain tension-controlled behavior, this test shows that a high amount of reinforcement ratio can significantly increase the cracking strength of concrete. A similar result was reported by Shah (1991) which showed that a very high cracking strength of concrete can be obtained if a high volume fraction of fibers (about 15%) is used. This is because when the fiber amount reaches a certain critical threshold, they can effectively carry the force and prevent concrete's microcracks from growing and interconnecting to form a percolation crack (Balaguru and Shah, 1992). It is believed that a high reinforcing bar ratio provides the same effect.

Table 1. Four-point loading specimens' information



R0	R5
No rebars	5 #3 rebars
$\rho_{TA} = 0\%$	$\rho_{TA} = 14\%$
$P_{cr} = 3.0$ kips (13.35 kN)	$P_{cr} = 9.1$ kips (40.48 kN)
$f_r = 1.5$ ksi (10.3 MPa)	$f_r = 3.3$ ksi (22.8 MPa)

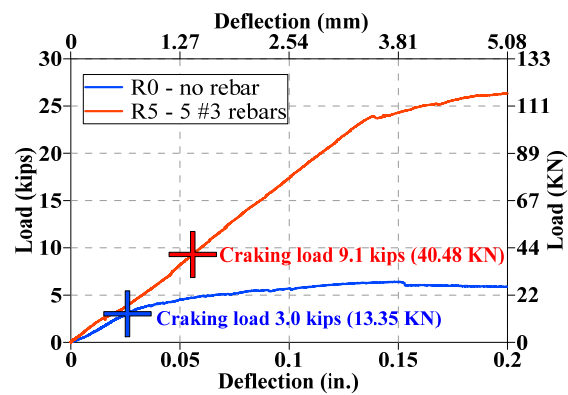


Figure 2. Load vs. deflection diagram for four-point loading tests

Allowing a higher amount of reinforcing bars leads to smaller stress in tensile reinforcement even at a higher load. Because crack widths in concrete beams are roughly proportional to the stress in steel reinforcement, the low stress will allow better control of the crack width and, hence, stiffness of the member. When the steel stresses are kept low under the service load, the accompanying low strains in the concrete and steel will produce only small rotations of the cross sections along the member, which translates into a small deflection (Nilson 1987).

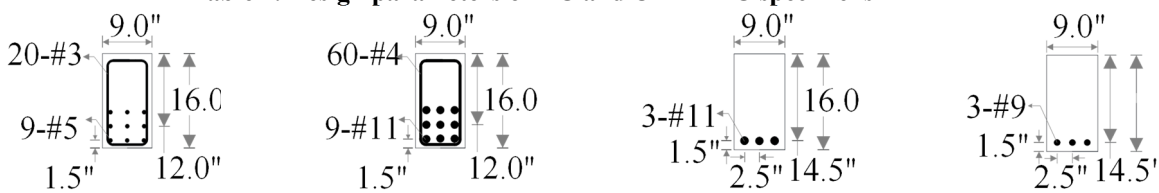
4. Large-Scale Experimental Verification

4.1 Specimen Design

Four simply supported beams, one made of reinforced concrete (RC) and three made of UHP-FRC were monotonically loaded to failure. All beam specimens had a width of 9 in. (229 mm), a height of 16 in. (406 mm), and a span length of 134 in. (3404 mm). A 20-in. (508 mm) constant moment region was at the mid-span of all specimens. Table 2 lists the design parameters of beams used in this experimental program. Specimens RC and UHP-FRC #1 used ASTM A615 reinforcing bars, while Specimens UHP-FRC #2 and UHP-FRC #3 used ASTM A1035 high-strength corrosion-resistant low-carbon chromium reinforcing bars to reduce the reinforcement congestion. To investigate the shear capacity of UHP-FRC in flexural members no shear reinforcement was used in Specimens UHP-FRC #2 and UHP-FRC #3.

The RC beam was designed to have the highest amount of longitudinal reinforcement while still maintaining tension-controlled behavior based on ACI 318 (2014) and AASHTO LRFD (2017) provisions. In other words, the extreme tensile reinforcement reached a 0.005 strain when the maximum concrete strain was 0.003. This led to the use of nine No. 5 reinforcing bars, corresponding to a flexural reinforcement ratio of $\rho = 2.58\%$ (Table 2). Shear reinforcement was provided outside of the constant moment region to ensure that failure was not governed by shear before reaching the ultimate flexural strength. Design compressive strength of the RC beam was 5,000 psi (34.5 MPa). The design compressive strength of UHP-FRC was 22 ksi (152 MPa) and the maximum usable compressive strain, ϵ_{cu} , was taken as 0.015. The flexural reinforcement ratio for specimen UHP-FRC #1 with Gr. 60 reinforcing bars was five times that of the RC beam which resulted in a ratio of $\rho = 13\%$, corresponding to nine No. 11 reinforcing bars (Table 2). The reinforcement areas were considerably reduced in specimens UHP-FRC #2 and UHP-FRC #3 with Grade 100 reinforcing bars. To simplify the design, the β_1 factor was assumed the same for plain concrete as recommended by ACI 318 and AASHTO LRFD. Neglecting the contribution of UHP-FRC on the tension side, which is a conservative assumption for design, it was calculated that the tensile strain of the extreme reinforcing bars in the UHP-FRC #1 beam was much larger (0.013) than the tension-controlled limit (0.005), even with a considerably higher reinforcement ratio.

Table 2. Design parameters of RC and UHP-FRC specimens



Specimen	Effective depth (d), in. (mm)	a/d	ρ (%)	V_f (%)	Targeted, f'_c (ksi) (MPa)	Measured, f'_c (ksi) (MPa)
RC1	12.0 (305)	4.75	2.58 (60S)	0	5 (35)	5 (35)
UHP-FRC #1	12.0 (305)	4.75	13.0 (60S)	3.0	22 (152)	21 (145)
UHP-FRC #2	14.5 (368)	3.93	3.59 (100S)	3.0	22 (152)	20.8 (143)
UHP-FRC #3	14.5 (368)	3.93	2.30 (100S)	3.0	22 (152)	20.8 (143)

4.2 Experimental Results

In the RC beam, the first flexural crack was observed at a stress on the tension side nearly equal to the modulus of rupture of the concrete (load: 12.0 kips or 53 kN). However, in UHP-FRC #1, the first visible flexural crack was not traced until 120 kips loading. The load versus deflection curve in Figure 3a shows that the slope changed very slightly at about 60 kips (267 kN), which is conservatively considered the first cracking load. Nevertheless, UHP-FRC #1 exhibits a nearly linear uncracked behavior up to 250 kips (1112 kN), thereby maintaining a very high stiffness up to 80% of the peak strength. As shown in Figure 1, the average concrete’s compressive strains in the RC and UHP-FRC #1 beams at their peak strength were measured by a DIC system as 0.003 and 0.015, respectively. The maximum measured strains were 0.006 and 0.025, respectively, for RC and UHP-FRC #1. This indicates that using a strain ($\epsilon_{cu} = 0.015$) to design a UHP-FRC beam provides a sufficient safety margin. The ultimate strength of the UHP-FRC #1 beam is 318 kips (1415 kN), which is 4.4 times that of an RC beam (72 kips or 320 kN). Figure 3a also shows that the UHP-FRC #1 beam had ample ductility, even with a reinforcement ratio five times greater than that of the RC beam. This indicates that using UHP-FRC in flexural members can largely increase

the strength and stiffness while maintaining a small self-weight. In fact, because the overstrength of the UHP-FRC beam beyond the design load (approximately 60 kips [267 kN]) is very large, the ductility capacity becomes less critical. Figure 3b and 3c show that the visible cracks in the UHP-FRC #1 beam are very small even at a very high load of 300 kips (1,334 kN).

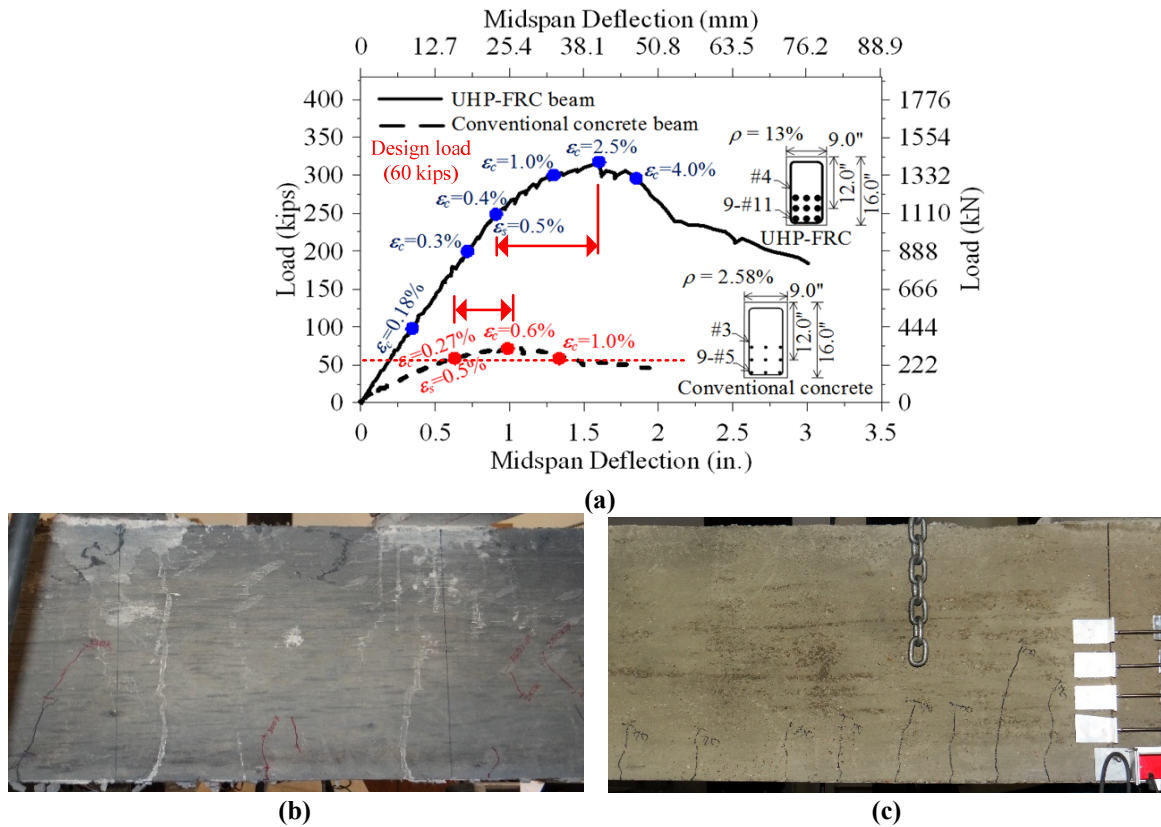


Figure 3. (a) Load vs. mid-span deflection responses of RC and UHP-FRC #1 beams, (b) observed cracks in UHP-FRC #1 beam at 300-kip (1334 kN) load, and (c) observed cracks in RC beam at 70-kip (311 kN) load

Strain gauge data indicates that the strains in the bottom reinforcing bars in the UHP-FRC #1 beam all reached 0.013, which is well beyond the tension-control limit of 0.005. At the 0.005 strain in longitudinal reinforcing bars, the concrete compressive strain observed in the UHP-FRC #1 beam was 0.004, which was much less than the design compressive strain of $\epsilon_{cu} = 0.015$. At the assumed first cracking of 60 kips (267 kN), the strains in the reinforcing bars were approximately 0.0005, corresponding to a stress of 14.5 ksi (100 MPa). Since conventional ASTM A615 reinforcing bars typically exhibit a fatigue endurance limit (1×10^6 cycles) at a stress range of approximately 24 ksi (166 MPa) (Wight, 2016), it indicates that UHP-FRC #1 can carry a full service live load of up to about 100 kips (445 kN) without fatigue concern. This loading is greater than the RC beam's ultimate load. On the other hand, in the RC beam, all reinforcing bars reached 60 ksi (414 MPa) at a load of approximately 50 kips (222 kN). Specimen UHP-FRC #1 remained at nearly a "pseudo" uncracked state up to nearly 90% of the peak load. The beam showed a very large deflection with a few small flexural cracks. This behavior is very different from the conventional RC beams, and indicates a significant synergetic action and tension-stiffening effect between the reinforcing bars and UHP-FRC in carrying the tensile stresses.

UHP-FRC #2 and UHP-FRC #3 were designed to intentionally fail in shear. For UHP-FRC #2, the first visible flexural crack was observed at 60 kips (267 kN). This approximately matches

the point where the stiffness of the load vs. deflection curve starts decreasing (Figure 4b). A critical web shear crack was developed at 150 kips (667 kN) (shear stress: $4.0\sqrt{f'_c}$ (577 psi)). At an ultimate load of 163 kips (725 kN) (shear stress: $4.5\sqrt{f'_c}$ (650 psi)), the web shear crack quickly propagated toward the loading point and support, eventually causing dowel failure along the bars. For UHP-FRC #3, the first visible flexural crack was observed at 50 kips (222 kN). This approximately agrees with the point where the stiffness of the load vs. deflection curve started decreasing (Figure 4b). A critical web shear crack also appeared at 150 kips (667 kN) (shear stress: $4.0\sqrt{f'_c}$ (577 psi)), and the beam failed at an ultimate failure load of 179 kips (796 kN) (shear stress: $4.9\sqrt{f'_c}$ (710 psi)) due to the loss of shear and dowel capacity. Load deflection and cracking behavior of UHP-FRC #3 is very similar to UHP-FRC #2 except for the fact that UHP-FRC #3 had a slightly better bond strength and dowel performance due to the smaller diameter of the bars.

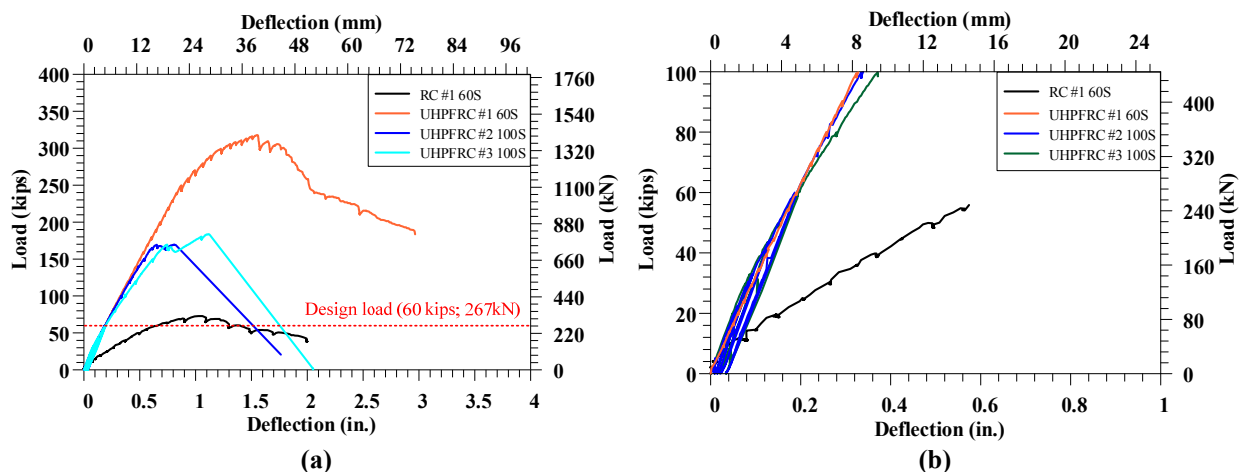


Figure 4. Load vs. deflection: (a) entire curves and (b) up to 100 kips (445 kN)

Strain gauge data indicates that the steel stress after cracking (about 60 kips or 267 kN) in Specimens UHP-FRC #2 and UHP-FRC #3 was approximately 24 ksi (166 MPa). Experiment results reported by DeJong and MacDougall (2006) indicated that ASTM A1035 high-strength corrosion-resistant low-carbon chromium reinforcing bars exhibit a fatigue endurance limit (1×10^6 cycles) at a stress range of approximately 45 ksi (310 MPa). Thus, the ASTM A1035 reinforcing bars' superior fatigue resistance can allow a full-service load up to approximately 120 kips (534 MPa) which is 10 times that of the RC beams' cracking load.

5. Finite Element Study of a 250-ft-long Bridge with UHP-FRC DBT Girders

From the large-scale testing of UHP-FRC flexural members, it was observed that UHP-FRC has a very high flexural cracking strength. The f_r for each specimen was calculated using its transformed section properties. The results are listed in Table 3. These f_r values are similar to that obtained from the small specimen shown in Table 1. The high f_r of UHP-FRC in highly reinforced flexural members allows eliminating prestress in bridge girders. While the cracking in prestressed concrete girders is controlled by prestress, reinforced UHP-FRC girders' crack control is based on high cracking strength and section modulus of the beam. In fact, the cracks are well controlled even after the first cracking due to the bridging effect provide by the fibers and high amount of reinforcing bars. This type of new non-prestressed girders is achieved by utilizing the unique mechanical characteristics of UHP-FRC and a new "ductile-concrete strong-reinforcement (DCSR)" design concept. The synergistic interaction of UHP-FRC and a high amount of

reinforcement allows the member to remain uncracked under the service load. The uncracked section keeps the deflection small. Additionally, the high compressive ductility of UHP-FRC guarantees a ductile failure of the member at ultimate loading. Using UHP-FRC with high-strength corrosion-resistant reinforcing bars can create a non-prestressed girder that not only provides all the advantages of a conventional precast prestressed concrete girder but also possesses other merits, which can eliminate issues that prestressed concrete girders encounter.

Table 3. Cracking moments and corresponding f_r of RC and UHP-FRC specimens

Specimen	Cracking load, kips (kN)	Cracking Moment, kip-inch (kN-m)	ρ_{TA} (only bottom layer rebars are used for the calculation)	First cracking strength, f_r , ksi (MPa)
RC	12 (53)	342 (39)	---	0.76 (5.24)
UHP-FRC #1	60 (267)	1,710 (193)	17%	3.18 (21.92)
UHP-FRC #2	60 (267)	1,710 (193)	17%	3.2 (19.17)
UHP-FRC #3	50 (222)	1,425 (161)	11%	3.0 (18.41)

To verify the DCSR design concept, a 250-ft (76.2 m) long bridge with a modified DBT section was analyzed using finite element analysis (FEA) with AASHTO dead and live loads. Girders designed with the DCSR concept typically have a large overstrength for ultimate strength. Hence, the design is controlled at the full-service load level to have the tensile stress at the bottom fiber of the girder less than its cracking strength. To satisfy the design requirements at the service loads (AASHTO Service-I and Service-III Limit States), eight optimized non-prestressed UHP-FRC DBT girders were used for the 50-ft (15.2 m) wide bridge. Because the limiting criteria in the design is the tensile stress of the girder at the bottom layer, the section dimensions were optimized based on FEA to lower the neutral axis. A cracking strength of 3 ksi (20.7 MPa) was used because experimental test results indicated that it can be reached as long as the cracking-control longitudinal reinforcement (the bottom layer of the rebars) ratio, ρ_{TA} , is at least approximately 15%. To provide the minimum ρ_{TA} , 22 No. 11 Grade 100 rebars were used ($\rho_{TA} = 15.25\%$). These bars can be easily placed at the bottom of the girder (Figure 5). The girders meet the service load requirements. In addition, the nominal moment capacity of the section is 898,812 kip-in. (101,552 kN-m), which is more than twice the factored moment demand of 404,222 kip-in. (45,671 kN-m). Using the shear capacity of UHP-FRC from the large-scale test results, these girders do not require any shear reinforcement. However, a minimum shear reinforcement as per ACI and AASHTO provisions should be used.

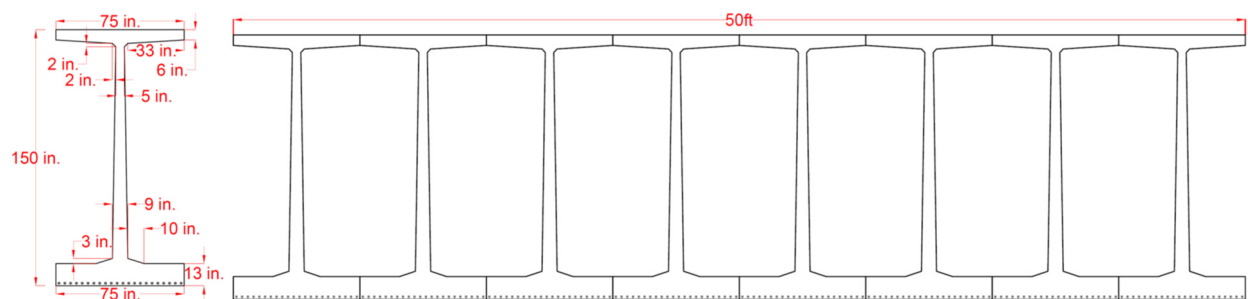


Figure 5. Prototyp 250-ft long non-prestressed UHP-FRC DBT girders (1 in. = 2.54 cm; 1 ft = 30 cm)

Table 4. Section information of 250-ft (76.2 m) long non-prestressed UHP-FRC DBT girder

Section properties	Height in. (cm)	Height of web in. (cm)	Flange width in. (cm)	Area in. ² (cm ²)	Inertia in. ⁴ (cm ⁴)	y_{bottom} in. (cm)	Weight kip/ft (Kg/m)
DBTM-150	150 (381)	126 (320)	75 (190.5)	2446.5 (15784)	8,207,556 (37,411,405)	61.25 (155.6)	2.55 (3787)

6. Economics

From an economic point of view, high-performance and high-strength materials have a much higher unit cost. Nevertheless, the economics of using the proposed new precast UHP-FRC girders can be justified by: 1) No additional materials or equipment such as prestressing anchorages, hydraulics for draping, and tensioning prestressing strands are needed; 2) No labor is needed for draping, tensioning, debonding, and cutting the strands; moreover, no prestressing quality control persons are needed. 3) Multiple casts can be made per day due to the high early strength of UHP-FRC (10 to 12 ksi within 24 hours); 4) Elimination can be achieved of most of shear reinforcement and all confining reinforcement at girder ends. No cracking control reinforcement is needed at the girder ends. 5) No prestress losses and camber issues occur. The elimination of camber deflection eliminates the on-site labor problems of lining up skewed DBT girders due to bridge deck profile problems. This advantage reinforces the need for the use of deck bulb-tee girders because it accelerates bridge construction, which provides a significant reduction in both time and labor. 6) Lower life-cycle costs are due to the sustainability of UHP-FRC. 7) Eliminating prestressing allows any precast plant to produce bridge girders even if it has no prestressing facilities. It also allows UHP-FRC bridge girders to be built onsite for long-span bridges, which resolves the difficult and costly transporting conventional long-span prestressed girders. In addition, it allows curved concrete girders to be built for bridges with horizontally curved alignments.

7. Conclusions

1. This study investigated a new precast UHP-FRC bridge girder made with non-prestressed high-strength corrosion-resistant reinforcing bars. Experimental results show that the new girder can be used to replace conventional precast, prestressed concrete girders with potential economic savings and long-term sustainability. Similar to the advantages of prestressed concrete over conventional reinforced concrete (Freyssinet, 1936), this study shows that non-prestressed UHP-FRC members offer the following advantages:
 - A considerable reduction in deformation (deflection);
 - Complete suppression of cracks in the concrete under service load; hence, cracks remain very small and have nearly no influence on the flexural stiffness of the member;
 - Higher compressive strength and ductility allow more reinforcing bars to be placed, which significantly increases moment capacity, cracking control, and fatigue resistance;
 - A high shear strength provided by UHP-FRC, which can considerably reduce the required shear reinforcement;
 - Substantial resilience with the ability to close temporary cracks after the overload is removed.
 - No issues related to prestressing such as prestress losses, end zone cracking, and camber.
 - High corrosion-resistance and long-term durability.
2. The concept of replacing prestressed concrete bridge girders with 250-ft (76.2 m) long non-prestressed UHP-FRC girders is demonstrated with the design of UHP-FRC deck bulb-tee girders. The new girders provide high first-cracking resistance and greater ultimate strength than conventional precast, prestressed deck bulb-tee girders. The design is straightforward with simpler shear design and longitudinal reinforcement detailing and does not have to consider cracking control reinforcement and complicated computation regarding long-term prestress loss and camber.

8. References

- AASHTO. (2017). LRFD Bridge Design Specifications. 8th edition, American Association of State Highway and Transportation Officials (AASHTO), Washington, D.C.
- ACI Committee 318. (2014). Building Code Requirements for Structural Concrete (ACI 318-14) and Commentary (ACI 318-14), American Concrete Institute, Farmington Hills, Michigan.
- Aghdasi, P., Heid A.E., and Chao, S.-H. (2016). “Developing Ultra-High-Performance Fiber-Reinforced Concrete for Large-Scale Structural Applications,” *ACI Materials Journal*, V. 113, No. 5, September-October 2016, pp. 559-570.
- Ahlborn, T., Harris, D., Misson, D., and Peuse, E. (2011). “Characterization of Strength and Durability of Ultra-High-Performance Concrete Under Variable Curing Conditions,” *Transportation Research Record: Journal of the Transportation Research Board*, No. 2251, Transportation Research Board of the National Academies, Washington, D.C., 2011, pp. 68–75.
- Balaguru, P. N. and Shah, S. P. (1992). *Fiber-reinforced Cement Composites*. McGraw-Hill, 530 pages.
- Chao, S.H.; Liao, W.C.; Wongtanakitcharoen, T.; and Naaman, A.E. (2007). “Large Scale Tensile Tests of High Performance Fiber Reinforced Cement Composites,” *High Performance Fiber Reinforced Cement Composites: HPFRCC-5*, International Workshop, Mainz, Germany.
- DeJong, S.J., and MacDougall, C. (2006). “Fatigue Behaviour of MFMX Corrosion-Resistant Reinforcing Steel,” *Proceedings of the 7th International Conference on Short and Medium Span Bridges*, Montreal, Canada.
- Federal Highway Administration (FHWA). (2011). “Ultra-High Performance Concrete,” *TechNote, FHWA-HRT-11-038*, Federal Highway Administration, 8 pages.
- Freyssinet, E. (1936). “A Revolution in the Technique of the Utilisation of Concrete,” *The Structural Engineer*, V. 14, No. 5, May 1936, pp. 242-259.
- Grubb, J.A., Blunt, J., Ostertag, C.P., and Devine, T.M. (2007). “Effect of Steel microfibers on Corrosion of Steel Reinforcing Bars,” *Cement and Concrete Research*, V. 37, pp. 1115-1126.
- Horii, H. and Nemat-Nasser, S. (1985). “Compression-Induced Microcrack Growth in Brittle Solids: Axial Splitting and Shear Failure,” *Journal of Geophysical Research*, V. 90, No. B4, pp. 3105-3125.
- Leonhardt, F. (1964). *Prestressed Concrete—Design and Construction*. Second Edition. Wilhelm Ernst & Sohn. 677 pages.
- Lin, T.Y., and Burns, N.H. (1981). *Design of Prestressed Concrete Structures*. Third Edition. John Wiley & Sons. 646 pages.

Naaman, A.E. (2012). *Prestressed Concrete Analysis and Design—Fundamentals*. Third Edition, Techno Press 3000. 1176 pages.

National Cooperative Highway Research Program (NCHRP). (2009). *Guidelines for Design and Construction of Decked Precast, Prestressed Concrete Girder Bridges*. Project No. 12-69.

Nilson, A.H. (1987). *Design of Prestressed Concrete*. Second Edition. John Wiley & Sons. 592 pages.

Precast/Prestressed Concrete Institute (PCI). (2011). *Bridge Design Manual*. Third Edition.

Shah, Surendra P. "Do fibers increase the tensile strength of cement-based matrix?." *Materials Journal* 88.6 (1992): 595-602.

Wight, J.K. (2016). *Reinforced Concrete—Mechanics and Design*. Seventh Edition. Pearson, 1144 pages.

9. Acknowledgments

This research was supported by the U.S. National Science Foundation under Award No. CMMI-1414391.